Korean J. Chem. Eng., **29**(7), 862-867 (2012)
DOI: 10.1007/s11814-011-0255-6

Heat transfer in a swirling fluidized bed with geldart type-D particles

Mohd Faizal Mohideen*,*,†, Binod Sreenivasan**, Shaharin Anwar Sulaiman***, and Vijay Raj Raghavan*****

*Faculty of Mechanical & Manufacturing Engineering, Universiti Tun Hussein Onn Malaysia, 86400 Batu Pahat, Johor, Malaysia
**Department of Mechanical Engineering, Indian Institute of Technology Kanpur, 208016, India
***Department of Mechanical Engineering, Universiti Teknologi Petronas, 31750 Tronoh, Perak, Malaysia
(*Received 10 June 2011 • accepted 2 October 2011*)

Abstract−A relatively new variant in fluidized bed technology, designated as the swirling fluidized bed (SFB), was investigated for its heat transfer characteristics when operating with Geldart type D particles. Unlike conventional fluidized beds, the SFB imparts secondary swirling motion to the bed to enhance lateral mixing. Despite its excellent hydrodynamics, its heat transfer characteristics have not been reported in the published literature. Hence, two different sizes of spherical PVC particles (2.61 mm and 3.65 mm) with the presence of a center body in the bed have been studied at different velocities of the fluidizing gas. The wall-to-bed heat transfer coefficients were measured by affixing a thin constantan foil heater on the bed wall. Thermocouples located at different heights on the foil show a decrease in the wall heat transfer coefficient with bed height. It was seen that only a discrete particle model which accounts for the conduction between the particle and the heat transfer surface and the gas-convective augmentation can adequately represent the mechanism of heat transfer in the swirling fluidized bed.

Key words: Swirling Fluidized Bed (SFB), Geldart Type D Particles, Heat Transfer Coefficient, Superficial Velocity

INTRODUCTION

In fluidization solid particles are transformed into fluid-like state through suspension in a gas or liquid. This method of contacting between solid and fluid has some unusual characteristics, and fluidization engineering puts them to good use [1]. The basic mechanism of a fluidized bed can be seen simply as fluid percolation through particle interstices via a distributor, in which particles begin to exhibit fluid-like characteristics upon experiencing sufficient drag force by the fluid. A large number of industrial processes use the fluidization technique in their daily operations: combustion, gasification of solid fuels, drying of particles, particle heating, oxidation, metal surface treatments and catalytic and thermal cracking [2,3].

The swirling fluidized bed features an annular bed and inclined injection of gas through the distributor blades, which then imparts the swirling motion to the bed [4]. This secondary motion inside the bed promotes better mixing and good solid-fluid contact - the most desired features in a fluidized bed. The construction of a swirling fluidized bed is shown in Fig. 1.

As the jet of gas enters the bed at a certain small angle, θ, to the horizontal plane, the jet will have two components of velocity. The vertical component of the jet velocity, which is given by V sin θ, will create fluidization of particles, while the horizontal component, V cos θ, will create swirling [4]. The distributor used in this bed consists of overlapping blades that are truncated sectors of a circle forming an annular region for gas flow. The cone in the center of the bed avoids a dead zone while gradually increasing the cross-sectional area of gas flow to the free surface above the bed.

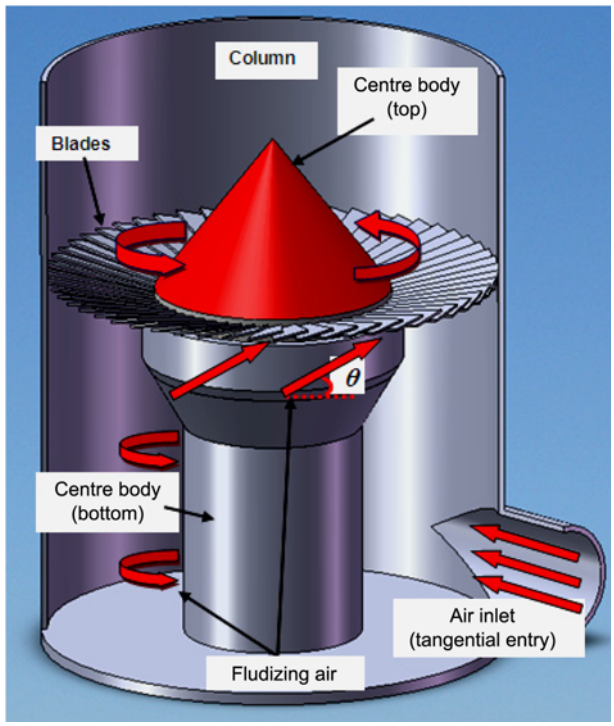

Fig. 1. Basic configuration of a swirling fluidized bed.

Many of the early works on wall-bed heat transfer in fluidized beds held that the principal resistance to heat transfer is a fluid film and that moving fluidized particles acting as turbulence promoters scour the film to reduce the resistance. The solid particle-surface contact is neglected and heat is assumed to flow from the surface

†To whom correspondence should be addressed.
E-mail: mfaizal@uthm.edu.my

to the air-solids mixture across the film at a rate many times higher than that which would exist if only air were moving through the column. All these models involve a steady state concept of the heat transfer process.

Gelperin and Einstein [5] proposed a model similar to that of Baskakov [6], and assumed that there is a zone of high porosity near the wall, of thickness $d_p/2$, which presents an additional thermal resistance. This surface resistance is empirically found to be expressed as a constant times the ratio of the particle diameter to the fluid thermal conductivity. The instantaneous thermal resistance of the packet of particles coming into contact with the surface is given by:

$$R_a = \sqrt{\pi t_c / \lambda_e C_s \rho_b} \quad (1)$$

where, t_c=contact time of the particle at the wall, λ_e=thermal conductivity of the emulsion and c_s=specific heat of the solid particles. The instantaneous heat transfer coefficient is subsequently evaluated.

From the work of Korelev et al. [7], it is well-known that the structure and, specifically, the porosity of a fixed and fluidized granular bed are different, adjacent to and at some distance from, a boundary wall; they determined the porosity of a fluidized bed near a wall experimentally by means of X-ray radioscopy and suggested an expression for the same. The approach taken by [8] retained the continuum concept of the emulsion right up to the heat transfer surface, but the effective thermal conductivity and heat capacity of the emulsion were taken as variable within one particle diameter of the surface. The authors felt that though the concept of a time-independent contact resistance was a good first approximation, the physical reasoning behind it was somewhat tenuous. All property variations were described in terms of the voidage variations in the vicinity of the constraining surface which are modeled from simple geometric considerations. It is assumed that the variation of voidage is confined to the plane normal to the wall. This variable property continuum model was solved numerically to obtain the Nusselt number as a function of Fourier number. Nu at very small Fourier numbers was obtained using a similarity solution method:

$$Nu = \frac{3^{2/3}}{2\Gamma(4/3)}\left[\frac{\lambda_e}{\lambda_g}\right]^{1/3} Fo^{-1/3} \quad (2)$$

where, $\Gamma(4/3)$ equals 0.89. Results were comparable with those from models composed of a uniform continuum and a surface resistance.

[9,10] Advocated the discrete particle model wherein attention is directed to the conduction resistance between the surface and the particles immediately adjacent to it. A realistic model of the detailed surface geometry near the points has been included. The emulsion cannot be modeled as a continuum with particle diameters exceeding 400 μm and especially in systems with short particle contact times. It is argued that the use of a gas film separating the surface from the first row of particles is not physically realistic. For spherical particles, a value of 12 has been recommended for the time-averaged conduction Nusselt number based on particle diameter. A major advantage of this model was that the exact value of the particle residence time at the surface was not required for the prediction of the heat transfer coefficient. At high Reynolds numbers in packed beds, it had been found that the conduction heat transfer from the wall to the first row of particles was augmented by the convection set up by lateral mixing of gas.

Cho et al. [11] reported the effects of gas velocity, solid circulation rate and particle suspension density on the bed-to-wall heat transfer coefficient in a circulating fluidized bed. The effect of heat transfer length on the particle convective heat transfer coefficient was also addressed based on experimental study conducted in a 0.1 m-ID, 5.3 m-high bed with 65 μm mean diameter FCC particles. They found that bed-to-wall heat transfer coefficient increases with solid circulation rate and decreases with gas velocity. Smaller particles were found to have higher heat transfer coefficient due to higher contact points to the wall. A correlation was also proposed by the authors to predict the heat transfer coefficient.

Grulovic et al. [12] studied the effect of particles on the wall-to-bed heat transfer (fluidized bed and flowing suspension) through experiments using spherical glass particles of 0.80-2.98 mm in diameter with water in a 25.4 mm inner diameter copper tube equipped with a steam jacket. In relating the wall-to-bed heat transfer with the friction between the heating wall and the liquid-solids fluidized bed, the authors reported the observation of two distinct flow regimes, a 'parallel regime' and 'turbulent regime', which are determined from a dimensionless number derived from the momentum equation. They concluded that the heat transfer coefficient is generally higher in turbulent regime and proposed a correlation, by treating the bed as a pseudo-fluid. A numerical and experimental study of unsteady heat transfer in fluidized bed was carried out by Hamzehei and Rahimzadeh [13]. Their CFD model utilized a multi-fluid Eulerian model which incorporates solid kinetic theory to simulate gas-solids flow. They reported bubble coalescing phenomena as per observation from simulation and discussed the influence of bed temperature on fluidizing gas temperature. The major finding was that when increasing gas velocity (hence higher heat transfer coefficient between gas and bed) the bed temperature decreased accompanied by increase of mean gas temperature, both occurring rapidly. For validation of their CFD model, the predicted pressure drops and gas temperature variations were compared with experimental data, and they concluded their model could predict hydrodynamics and heat transfer of gas-solid fluidized bed reasonably well.

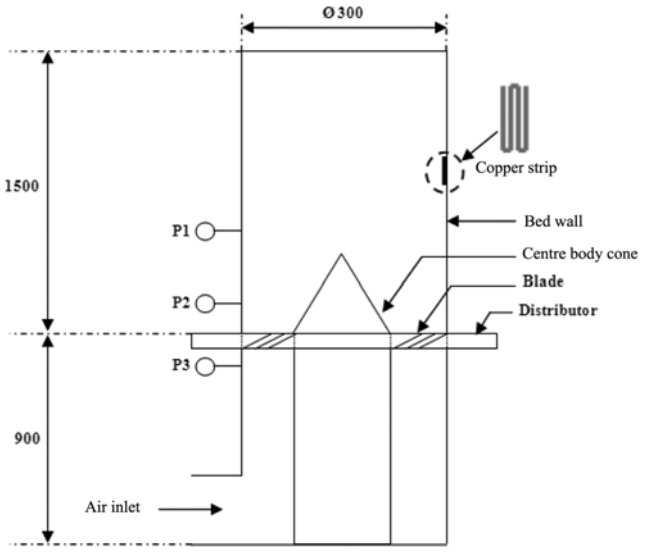

Fig. 2. Schematic diagram of the experimental set-up.

EXPERIMENTAL APPARATUS AND PROCEDURE

The schematic diagram of the test rig is given in Fig. 2. The unit consists of a Plexiglas column enclosing a Plexiglas cylinder that forms the bed wall. The column and the bed are mounted on the distributor. The annular spiral distributor used in this bed is a variant of the spiral distributor developed by Ouyang and Levenspiel [14]. But, unlike the spiral distributor, wherein overlapping blades shaped as full sectors of a circle were welded together at the center of the bed, the annular distributor is made of a number of blades that are truncated sectors of a circle [4]. Sixty such blades are arranged at an angle of 12° to the horizontal with the help of two Plexiglas outer and inner holders, by cutting slots in each holder. The inner holders are arranged around a Bakelite disk of diameter 200 mm at the center. The overlapping length between the blades directs the air at the designed angle. The gap between two blades is not uniform but varies in proportion to the radius, thereby creating a trapezoidal opening for air flow. The air gap for the present configuration is 1.18 mm at the inner radius and 2.27 mm at the outer radius.

A metal cone is centrally located at the base of the bed. In the presence of a cone at the bed center, the superficial velocity of the gas decreases continuously from the distributor to the free surface of the bed, owing to the increasing cross-section available for air flow. Hence, one could operate relatively deeper beds at high velocities without the problem of particle elutriation. The cone also eliminates the possible creation of a 'dead zone' at the center of the bed.

1. Temperature Measurement

To study the bed-wall heat transfer, a 50 μ thick constantan foil with the composition of Cu 60% and Ni 40% was used. The thermal conductivity of the constantan foil is 22.7 W/m K, while its electrical resistivity is 49 μΩ·cm at 20 °C. Fig. 3 shows the foil that was affixed on the wall of the fluidized bed column. Copper strips were soldered to the foil at the top and bottom edges to reduce the resistance to the flow of current. The actual locations of the thermocouple positions on the foil are also shown in Fig. 4. Type E Chromel-constantan thermocouples with 90% Ni & 10% Cr for chromel and 55% Cu & 45% Ni for constant were used. To measure the exit gas temperature, a traversing thermocouple probe was positioned so that its tip was just above the free surface of the bed.

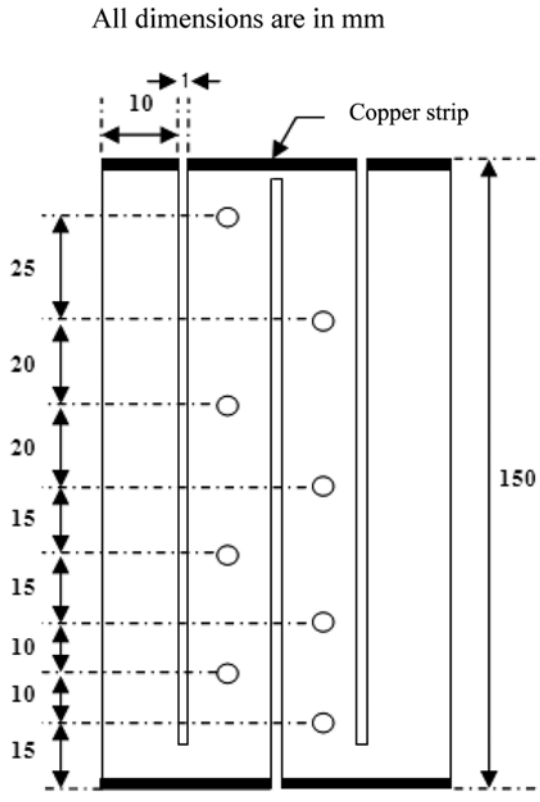

Fig. 3. Constantan heater foil and thermocouple location.

2. Experimental Procedure

The experiments were designed to bring out the effects of the following parameters on the wall-bed heat transfer coefficient:

(a) Superficial velocity of air (hence, the swirl velocity)

(b) Thermocouple position (or height of the bed as measured from the distributor level)

(c) Particle size

(d) Type of center-body: cone or cylinder.

Attention was focused mainly on the swirling mode of operation, because this regime is of maximum practical interest. Batch type experiments were carried out under the following conditions:

Bed weight (kg)	: 0.5, 0.75, 1.0, and 1.5
Particle diameter (mm)	: 2.61, 3.56
Centre-body	: cone
Superficial air velocity	: 1.8-3.5 m/s

Accurately weighed particles were poured into the bed and the air flow rate was increased till stable swirling began. The voltage readings corresponding to the different thermocouple positions were noted down from the voltmeter. Then the air flow rate was increased to a higher value. The expanded bed height at each superficial velocity was also observed. This gives the height of the foil immersed in swirling particles, which turns out to be an important factor influencing the variation of heat transfer coefficient with height of the bed. Since the energy input to the foil is kept a constant, a constant heat flux condition may be considered to exist. Assuming that the energy dissipated at any location is carried away by the swirling emulsion, the heat transfer coefficient, h, may be readily obtained from:

$$q''=h\,(T_{foil}-T_{bed}) \tag{3}$$

Knowing the voltage applied across the foil, the resistance of the foil and the surface area of the foil, the heat flux q″ can be calculated.

RESULTS AND DISCUSSION

The following sets of graphs were drawn based on the experimental data:

(a) Heat transfer coefficient vs. superficial velocity at different heights measured from the distributor level, for different bed weights, for a given particle size and centre-body.

(b) Heat transfer coefficient vs. height above the distributor at different air superficial velocities, for a given particle size and centre-body.

(c) Heat transfer coefficient vs. height above the distributor for a

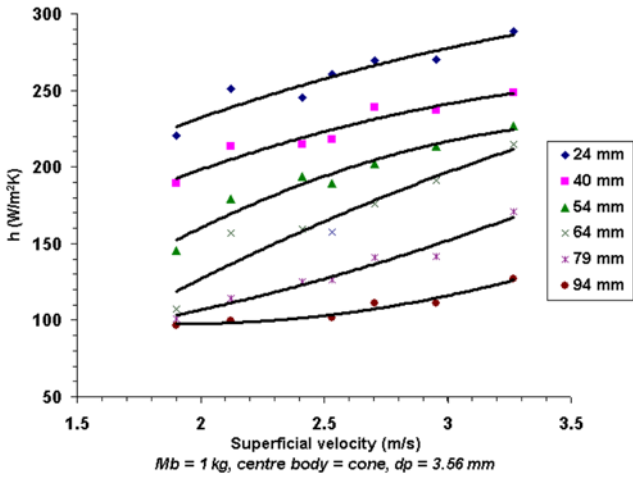

Fig. 4. h vs. U at different heights above the distributor.

cone and a cylinder at the centre of the bed, the particle size and velocity being kept constant.

Though a large number of graphs, many of them displaying similar trends, could be plotted from the data generated under each of the sets (a) to (c), only a few representative ones which bring out the typical behavior of the system are taken up for discussion in this section. The effect of the smaller particle size (2.61 mm) is also not discussed here for reasons of brevity.

1. Heat Transfer Coefficient (h) vs. Superficial Velocity (U)

In these graphs, three different trends can be identified depending on the thermocouple position above the distributor. Figs. 4 to 6 give typical h versus U plots for beds of different weights and with cone and cylinder as the center-bodies.

The h values corresponding to the thermocouples located closer to the distributor are of the highest magnitude as the angular velocity of air (as well as particles) is a maximum in this region. With the cone as the center-body, a maximum increase of 20% is observed as the velocity is varied from 2 to 3 m/s. In a 0.5 kg bed, the h vs. U curve corresponding to a location 19 mm from the distributor shows a maximum value of 340 W/m^{2}K at 2.8 m/s and thereafter decreases steadily to 270 W/m^{2}K at 3.7 m/s (which is even lower than the value at 2 m/s). This is so because, at velocities greater than

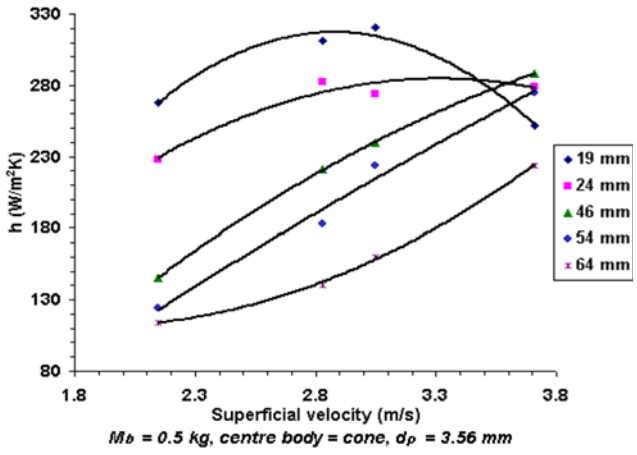

Fig. 5. h vs. U at different height above the distributor.

3 m/s, the thermocouple voltage in the region adjacent to the distributor increases due to fall in the particle concentration Fig. 5.

At high velocities, the thermocouple voltage close to the distributor is higher because the gas passes through the interstitial space by increasing the separation between particles. As the gas velocity turns more towards the vertical, as it will in a deep bed, the extra gas flow appears as bubbles and the interstitial space is not so large as it was lower down in the bed, where the vertical component vy is small. At lower air velocities, the particle convective component and the air convective component are both low. Particles of diameter 2.61 mm and 3.56 mm used in this work fall in the category of large particles with significant gas convection. However, since the bed voidage also increases simultaneously, the contribution of the population of particles decreases and the cumulative heat transfer, represented as the heat transfer coefficient, reaches a peak value and declines as a function of air velocity.

h vs. U curves display a more or less linear trend at intermediate thermocouple positions (45 mm to 75 mm, depending on the bed weight). This region of the foil is not "wetted" by particles at low velocities. As U increases, the bed expands and the foil gets progressively immersed in swirling particles. Initially, this region comes into contact with the free surface and subsequently with lower swirling layers of higher angular velocities. Also, the tangential component of the gas jet velocity (vθ) continuously increases at any layer of the bed. Hence, the steady increase in the heat transfer rate to the particles manifests as a steady increase in heat transfer coefficient. For a 0.5 kg bed, a 1 m/s rise in superficial velocity causes as much as an 80% increase in the value of h.

At heights ranging from 80 to 130 mm above the distributor, the region of the foil comes into contact with the swirling bed only at superficial velocities exceeding 3 m/s. In the lower velocity range of 2 to 2.5 m/s, h is practically a constant. Any minor increase should be attributed to the increase in velocity of air flowing past the foil. As velocity increases, the bed expands and due to intense swirling, a few particles which are thrown up the freeboard region impinge on the foil, resulting in a rise in the mean heat transfer coefficient. Beyond 3.5 m/s too, a steadily rising trend of the h-U curve should be expected. Thus, the behavior of the h vs. U curves is mainly influenced by the height of the foil immersed within the bed (ie., the expanded bed height). Table 1, gives the expanded bed heights at various superficial air velocities for a 0.75 kg bed of 3.56 mm particles, with cone as the center-body.

In the presence of a cylinder at the center of the bed, h is found to be practically invariant with velocity in the region just above the distributor. This is evident from Fig. 6. This result is at variance with the observations for a cone as center-body. In the case of a cylinder as the center-body, the bed weight per unit area is greater. To balance

Table 1. Expanded bed heights at various superficial air velocities (M_b=0.75 kg, d_p=3.56 mm)

Superficial velocities (m/s)	Immersed height of foil (mm)
2.2	55
2.4	60
2.55	65
2.7	75
2.9	80

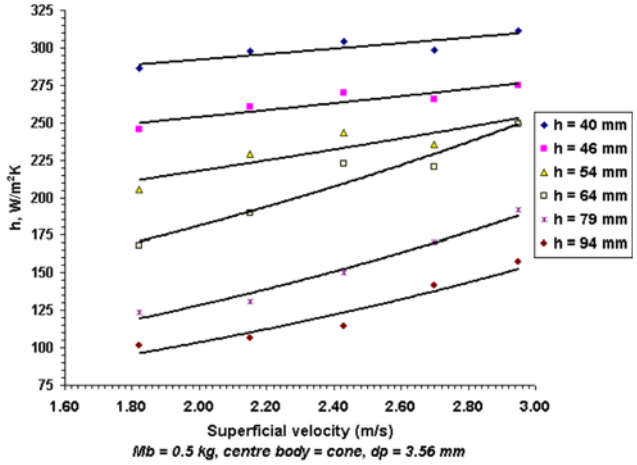

Fig. 6. h vs U at different heights above the distributor.

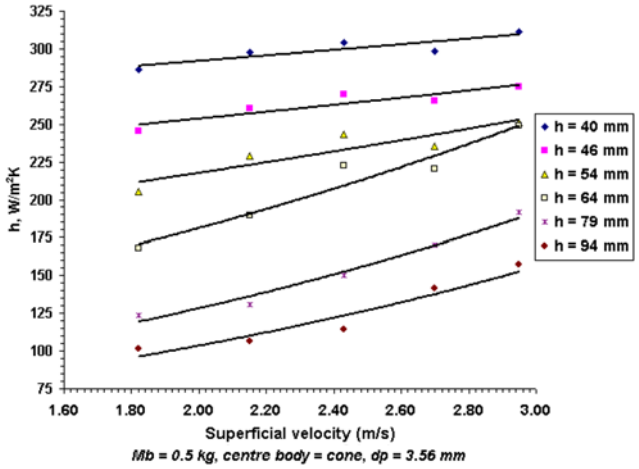

Fig. 8. h vs U at different heights above the distributor (for different particle sizes).

the larger downward force, a greater air drag is required on the particles. The air velocity is required to be greater, which implies smaller interstitial space and lower bed expansion. A simple-to-visualize explanation for the same phenomenon could be given; thus, the larger the bed height (bed weight per unit area), the greater is the downward compressive force and smaller the bed expansion.

2. Heat Transfer Coefficient (h) vs. Height Above the Distributor (H) at Different Velocities

A major conclusion that can be drawn from these graphs, Figs. 7 and 8, is that h decreases with height above the distributor. At U= 3 m/s, the h value at a height of 20 mm from the distributor is roughly twice the value at 80 mm. At lower bed weights of 0.5 and 0.75 kg, it has been inferred from visual observation of the bed that there cannot be too significant a variation in rotational velocity along the height of the bed to cause such a wide variation in heat transfer coefficient. The convective augmentation of the heat transfer coefficient is maximum in the region adjacent to the distributor, where the gas has the highest angular momentum. The contribution of the convective component would be the least at the free surface of the bed.

At a high velocity of 3.65 m/s in a 0.5 kg bed, h increases from the distributor level, reaches a peak value at a height of around 35 mm and thereafter declines steadily. While the fall in particle concentration is responsible for the lower h values adjacent to the distributor, the steadily decreasing convective component causes a decline above 35 mm.

When experiments were repeated with particles of diameters 2.61 mm, a higher heat transfer coefficient resulted with smaller particles (Fig. 8). A similar effect has been documented by [11] for small particles in a conventional fluidized bed. The reasons assigned were an increase in the number of contact points between particles and the surface and reduction in the transfer path length between the surface and the particle by which heat must flow by conduction through the gas phase. When the cylinder was used as the center-body, the heat transfer coefficient was higher than for a cone. Apparently, this is due to the higher average superficial velocity in the case of a cylinder at any given flow rate.

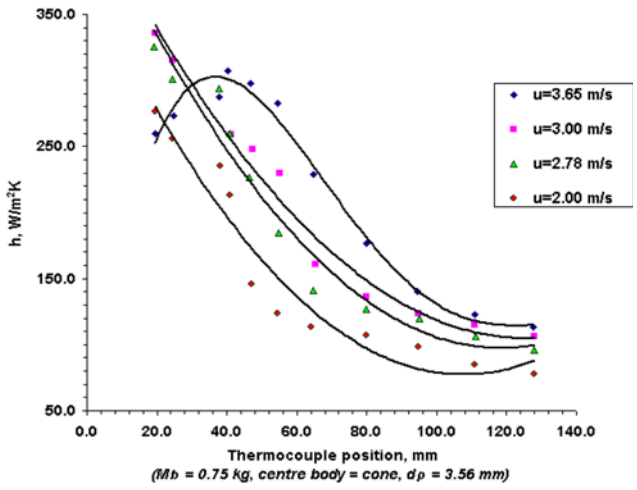

Fig. 7. h vs U at different heights above distributor.

CONCLUSION

Unlike a conventional fluidized bed, a swirling fluidized bed may have more than one regime of operation: incipient mode, partial swirling, stable swirling and two-layer fluidization regime for deeper beds. This paper addresses wall-bed heat transfer studies only in the swirling regime, to derive maximum advantage of the bed due to good particle turbulence. Thus, the bed appears to be more suited for operation in the shallow mode.

Three different trends have been identified in the h-U curves, depending on the location above the distributor level. The height of the foil immersed in the expanded bed height of the swirling bed turns out to be an important factor influencing the wall-bed heat transfer coefficient. In shallow beds with a cone as the center body, a maximum has been observed on the h-U curves in the region adjacent to the distributor at high velocities, the reason being a reduction in the particle concentration in this region as a consequence of bed expansion. The behavior of the h-H curves agrees with the visual observations made in a deep bed, wherein the tangential component of velocity is attenuated to zero at a certain height above the distributor, leaving only the vertical component to advance to the

top layer. Unlike in a conventional fluidized bed, the convective augmentation of heat transfer coefficient is not a constant value, but decreases continuously from the bottom to the free surface of the bed.

This study can be extended by varying the angle of injection of air and also by using different particle sizes and material. This may help to get a more complete picture towards understanding wall-bed heat transfer phenomena in a swirling fluidized bed. Heat transfer between the distributor and the bed can be studied by affixing a heater foil on one of the distributor blades. This may resolve the question of the degree of contact between particles and the distributor at various velocities.

ACKNOWLEDGEMENT

The authors wish to express their deepest gratitude to the Universiti Tun Hussein Onn Malaysia (UTHM), Universiti Teknologi Petronas (UTP) and the Ministry of Higher Education (MOHE), Malaysia for supporting this research under the Fundamental Research Grant Scheme (FRGS).

REFERENCES

1. D. Kunii and O. Levenspiel, *Fluidization engineering*, 2nd Ed., Butterworth-Heinemann (1991).
2. J. R. Howard, *Fluidized bed technology: Principles and applications*, Adam Hilger Publication, Bristol, U.K. (1989).
3. C. Amonsirirat, B. Chalermsimsuwan, L. Mekasut, P. Kuchontara and P. Piumsomboon, *Korean J. Chem. Eng.*, **28**(3), 686 (2011).
4. B. Sreenivasan and V. R. Raghavan, *Chem. Eng. Process.*, **41**, 99 (2002).
5. N. I. Gelperin and V. G. Einstein, Heat Transfer in Fluidized Beds, Academic Press, London (Edited by J. F. Davidson and D. Harrison), 99 (1971).
6. A. P. Baskakov, *Int. Chem. Eng.*, **4**(2), 320 (1964).
7. V. N. Korolev, N. I. Syromyatnikov and Tolmachev, *Inzhenerno-Fizicheskii Zhurnal*, **21**(6), 973 (1971).
8. J. Kubie and J. Broughton, *Int. J. Heat Mass Transfer*, **18**, 289 (1975).
9. N. A. Decker and L. R. Glicksman, *Int. J. Heat Mass Transfer*, **26**(9), 1307 (1984).
10. D. Gloski, L. R. Glicksman and N. A. Decker, *Int. J. Heat Mass Transfer*, **27**(4), 599 (1984).
11. Y. J. Cho, S. D. Kim and G. Y. Han, *Korean J. Chem. Eng.*, **13**(6), 627 (1996).
12. R. G. Grulovic, N. B. Vragolovi, Z. Grbavcic and A. Zorana, *Int. J. Heat Mass Transfer*, **51**, 5942 (2008).
13. M. Hamzehei and H. Rahimzadeh, *Korean J. Chem. Eng.*, **27**(1), 355 (2010).
14. F. Ouyang and O. Levenspiel, *Ind. Eng. Chem. Process Des. Dev.*, **25**, 504 (1986).